Electronic Energy Transfer

DOI: 10.1002/ange.200900188

Exploring the Limits of Förster Theory for Energy Transfer at a Separation of 20 Å**

Raymond Ziessel, Mohammed A. H. Alamiry, Kristopher J. Elliott, and Anthony Harriman**

Electronic energy transfer (EET) plays one of the key roles in natural photosynthesis, as it is primarily responsible for ensuring that the reaction-center complex is adequately supplied with photons,[1] and has found numerous important applications in artificial analogues. Most chemical systems, including photosynthesis, transfer photonic energy between relatively closely spaced centers where Förster-type dipole–dipole theory[2] might not be entirely valid. Indeed, there is a plethora of molecular donor–spacer–acceptor (D–Sp–A) systems where EET occurs by a through-bond mechanism. Often the two routes (that is, through-bond and through-space) run in parallel and it is difficult to elucidate the dominant effects for weakly coupled systems. This is a particularly challenging problem, which is exacerbated by growing doubts about the acceptability of calculating Förster rates from conventional theory.[3,4] Herein, we attempt to inhibit through-bond EET by incorporating an orthogonal connection into the spacer unit whilst modulating the overlap integral for through-space EET. A critical objective of the work is to make a quantitative assessment of how well Förster theory works for intramolecular EET across short (that is, 20 Å), rigid bridges. To better confront the theory, the orientation factor[5] has been varied by modification of the transition dipole moment vector for the acceptor.

Such a strategy is made possible by using a 2,2′-disubstituted-9,9′-spirobifluorene bridge as the starting point for the synthesis.[6] This template allows formation of asymmetric donor–spacer–acceptor systems (D–Sp–A; Scheme 1) by using various iodophenyl-substituted dyes and a racemic mixture of diethynylspirobifluorene.[7] Promotion of these cross-coupling reactions with Pd^0 catalysts facilitates the one-pot synthesis of BOD (30%; BOD is a regular boron dipyrromethane dye) and BOD–BOD (25%), or EXP (28%; EXP is an expanded boron dipyrromethane dye that absorbs at much lower energy) and EXP–EXP (25%) in respectable yields. The target BOD–EXP conjugate was conveniently prepared in 72% yield from BOD or EXP and the iodophenyl/boron dipyrromethane (Bodipy) counterpart by using similar protocols. The NMR spectra of these compounds, which display the individual contributions of each unit without obvious electronic perturbation, are well-defined, thus confirming the absence of aggregates.

The target compound BOD–EXP (Scheme 1) is a rigidly linked D–Sp–A molecule. The geometry around the bifluorene spacer provides for a perpendicular arrangement[6] where the two boron atoms are separated by 19.5 Å. Initial studies showed that the central spacer had no effect on the photophysical properties of either mono- or binuclear versions of BOD and EXP (Scheme 1) in acetonitrile or methyltetrahydrofuran (MTHF). The absorption spectrum recorded for BOD–EXP in CH_3CN shows well-resolved sets of transitions that can be readily assigned to the appropriate subunits by reference to the model compounds (Figure 1 and the Supporting Information).

Moreover, illumination of BOD–EXP at 635 nm leads to the selective formation of the first excited singlet state localized on the EXP moiety (Figure 1). Fluorescence from this subunit is centered at 780 nm; the fluorescence quantum yield (Φ_F) and lifetime (τ_S) remain highly comparable to those recorded for the model compounds under identical conditions (Table 1). Thus, the presence of BOD has no effect on the photophysical properties of EXP. In contrast, excitation of BOD–EXP in CH_3CN at 480 nm results in the selective population of the first excited singlet state resident on the BOD unit. Weak fluorescence can be detected at 540 nm and assigned to BOD by reference to the model compounds; in addition there is strong fluorescence from the EXP moiety. For the BOD component, both Φ_F and τ_S are decreased considerably relative to the reference molecules (Table 1), and it is clear that EET occurs from BOD to EXP under these conditions. The rate constant for EET (k_{EET}) can be calculated by comparison of the relevant lifetimes and has a value of $2.6 \times 10^9\ s^{-1}$. A similar rate constant ($k_{EET} = 2.4 \times 10^9\ s^{-1}$) was recorded in MTHF. In both solvents, the concept of efficient EET was confirmed by the close agreement between the absorption and excitation spectra and by the growth of EXP-localized fluorescence on relatively long timescales. The probability of EET, which occurs in competition with radiative and nonradiative decay of the excited singlet state of the donor, is approximately 90% under all conditions. It should be emphasized that whereas the optical transitions associated with BOD[8] are of π,π* character, those centered

[*] Dr. R. Ziessel
Laboratoire de Chimie Moléculaire et
Spectroscopies Avancées (LCOSA)
Ecole Européenne de Chimie, Polymères et Matériaux, CNRS
25 rue Becquerel, 67087 Strasbourg Cedex 02 (France)
E-mail: ziessel@chimie.u-strasbg.fr
Dr. M. A. H. Alamiry, K. J. Elliott, Prof. A. Harriman
Molecular Photonics Laboratory, School of Chemistry
Bedson Building, Newcastle University
Newcastle upon Tyne, NE1 7RU (UK)

[**] We thank the CNRS, EPSRC (EP/E014062/1), Université Louis Pasteur, and Newcastle University for financial support.

Supporting information for this article (synthesis and characterization of new compounds and methods used for the photophysical investigations; fluorescence quantum yields were measured with respect to a range of standards, as reported elsewhere[20]) is available on the WWW under http://dx.doi.org/10.1002/anie.200900188.

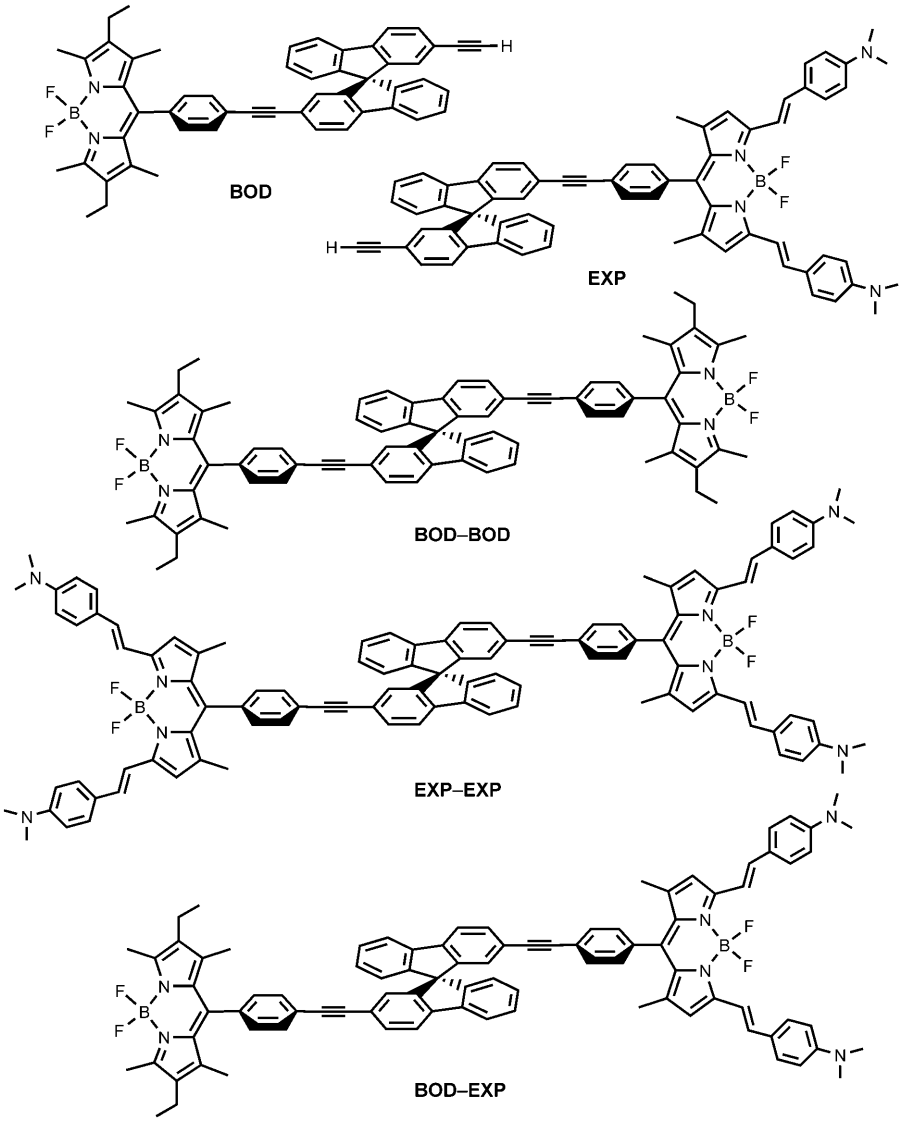

Scheme 1. Molecular formulae of the spiro-bridged Bodipy-based dyes.

on EXP comprise considerable charge-transfer interactions.[9] This change in orbital origin affects both the spectral profiles and the direction of the transition moment vectors. In both cases, the *meso*-phenylene ring serves to minimize both donor–acceptor orbital overlap and bridge-mediated energy transfer.

On the basis that only coulombic interactions occur, we can present k_{EET} in the form of Equation (1),

$$k_{EET} = \frac{|V_{CO}|^2 J_{DA}}{\hbar^2 c} \quad (1)$$

where V_{CO} is the electronic coupling matrix element[10] and J_{DA} is a form of the spectral overlap integral[11] that has units of cm. In this case, the individual spectral curves are normalized [Eqs. (2) and (3)]; f_D is

$$J_{DA} = A\,B \int \frac{f_D(\nu)}{\nu^3}\frac{e_A(\nu)}{\nu}\,d\nu \quad (2)$$

$$A \int \frac{f_D(\nu)}{\nu^3}\,d\nu = B \int \frac{e_A(\nu)}{\nu}\,d\nu = 1 \quad (3)$$

the fluorescence spectral profile for the donor and ε_A is the molar absorption coefficient for the acceptor. Now, V_{CO} for coulombic interactions can be expressed[12] in the form of Equation (4), where κ is

$$V_{CO} = \frac{s\kappa}{4\pi\varepsilon_0}\frac{|\mu_D||\mu_A|}{R^3} \quad (4)$$

the orientation factor, which allows

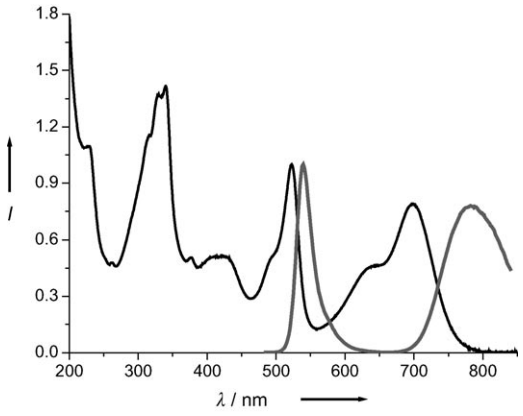

Figure 1. Absorption spectrum (black line) and normalized fluorescence spectra (gray lines) recorded for BOD–EXP in CH_3CN at 20 °C. Excitation was at 635 nm for EXP and 490 nm for BOD.

Table 1: Photophysical properties of the various spiro-based dyes in CH_3CN solution at 20 °C.

Cmpd[a]	λ_{ABS}[f] [nm]	λ_{FLU}[g] [nm]	Φ_F	τ_S [ns]
BOD	523	540	0.45	4.4
BOD–BOD	523	540	0.40	4.1
EXP	700	780	0.045	1.6
EXP–EXP	700	780	0.040	1.4
BOD–EXP[b]	525	540	0.033	0.35
BOD–EXP[c]	698	780	0.041	1.5
EXP($2H^+$)[d]	619	635	0.77	5.4
EXP–EXP($2H^+$)[d]	620	635	0.84	5.3
BOD–EXP($2H^+$)[b,d]	521	538	0.028	0.32
BOD–EXP($2H^+$)[c,d]	620	635	0.84	5.3
BOD–EXP(H^+)[b,e]	523	540	0.15	1.2
BOD–EXP(H^+)[c,e]	675	750	n.d.	2.2

[a] See Scheme 1 for molecular formulas. [b] Refers to the BOD unit. [c] Refers to the EXP unit. [d] Diprotonated EXP, after addition of a slight excess of HCl. [e] Monoprotonated EXP. [f] Absorption maximum. [g] Fluorescence maximum.

for multipole–multipole interactions, and μ_D and μ_A are the transition dipole moments for the donor and acceptor, respectively. The screening factor s can be expressed[13] in terms of Equation (5), where n is the refractive index of the

$$s = \frac{3}{2n^2 + 1} \quad (5)$$

solvent. Spectroscopic data were used to calculate values of 0.0015 cm, 4.5 D, and 7.6 D for J_{DA}, μ_D, and μ_A, respectively. The spectral overlap integral is kept modest by the relatively large energy gap, indeed fluorescence from BOD falls mostly within the wavelength range in which EXP is only weakly absorbing (Figure 1), despite the high oscillator strength of EXP. The average interchromophore separation R, taken as the center-to-center distance between the transition dipole vectors, has a value of 20.5 Å, according to molecular modeling studies (RHF 3-21G*) carried out in a reservoir of solvent molecules.

The orientation factor can be calculated from the transition dipole vectors for the two chromophores. For BOD, this vector is aligned with the long molecular axis but, because of charge-transfer interactions, the two identical vectors for EXP fall along the styryl groups. This arrangement gives rise to a reasonably high orientation factor ($\kappa^2 = 0.63$), which is similar to that for a random orientation ($\kappa^2 = 0.67$) of the chromophores. Now, the computed coupling element ($|V_{CO}| = (0.91 \pm 0.10)$ cm^{-1}) obtained from Equation (4) can be compared with the experimental value ($|V_{CO}| = 1.21$ cm^{-1}) derived by using Equation (1). The agreement is astonishingly good, with the most likely sources of error relating to uncertainties in κ and R, which are caused by the use of point dipoles, and to the accuracy in calculating the transition dipole moments of the donor and acceptor.[14] Usually, the value of V_{CO} is overestimated by using Förster theory, although cases to the contrary are known.[15] It is possible that, despite the poor conductance of the spacer, part of the discrepancy might be attributed to through-bond electron exchange. Before considering this latter possibility, however, we opted to measure the k_{EET} values over a modest temperature range.

In fluid butyronitrile (BuCN), the k_{EET} value decreases progressively upon lowering the temperature, but the effect is shallow and corresponds only to a twofold reduction in rate on cooling from 295 to 165 K. Arrhenius-type behavior is not observed. Below 150 K, where the solvent forms a glassy matrix, the rate is independent of temperature ($k_{EET} = 1.2 \times 10^9$ s^{-1}). Although the photophysical properties of BOD do not change significantly over this temperature range, there are pronounced differences for EXP (Figure 2). Between 295 and 185 K, both the absorption and fluorescence maxima of EXP move steadily to lower energy; at 185 K, $\lambda_{ABS} = 728$ nm and $\lambda_{FLU} = 795$ nm. This effect is caused by temperature-induced changes in the dielectric constant of the solvent; these decrease the J_{DA} value without affecting either the κ^2 or R values and give rise to the steady fall in the k_{EET} value. As BuCN starts to freeze, there is an abrupt hypsochromic shift for both absorption ($\lambda_{ABS} = 680$ nm) and emission ($\lambda_{FLU} = 755$ nm) maxima as the charge-transfer effect is minimized.

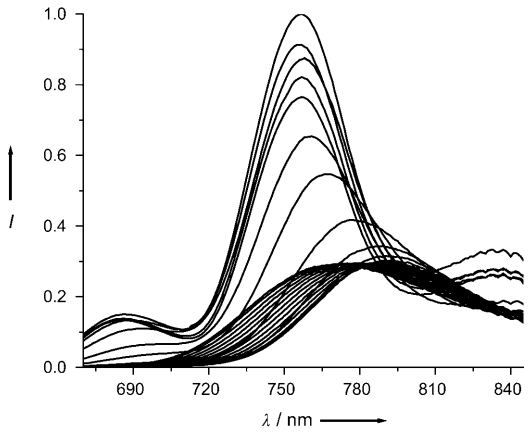

Figure 2. Fluorescence spectra recorded for BOD–EXP in BuCN as a function of temperature, following excitation into the EXP unit; temperatures cover the range 295–77 K (see text).

This shift causes an increase in the J_{DA} value, but a decrease in both the κ^2 and R values.[16] The variation in the k_{EET} value accurately reflects these changes, thereby confirming that only coulombic interactions need be considered and further emphasizing that simple Förster theory works well under these conditions. When establishing a quantitative match between observed and predicted rates, it is necessary to allow for temperature-induced changes in the refractive index of the solvent. Note that the fluorescence decay curves of both BOD and EXP remain monoexponential over this temperature range.

The above picture indicates an excellent agreement between the experimental and computed V_{CO} values, without the need for more elaborate data manipulation. It is possible that the errors tend to cancel in this system where the transition moment vectors are well-defined. To ensure against pure coincidence, however, we have extended the study to include two other D–Sp–A molecules where both the J_{DA} and κ^2 values are expected to change but the geometry remains intact. Fortunately, this situation is easily realized for BOD–EXP. Thus, titration of EXP with HCl in CH_3CN solution leads to protonation of both tertiary nitrogen atoms[17] and serves to curtail the intramolecular charge-transfer interactions. Protonation occurs over two well-resolved steps, with (effective) pK_{A1} and pK_{A2} values of 5.2 and 3.0, respectively, in CH_3CN. Because of the disparate pK_A values, it is possible to study EET to the mono- and diprotonated EXP dyes as they display very different optical properties.[17]

Firstly, we focus on the diprotonated dye EXP($2H^+$). In the presence of a slight excess of HCl, its absorption maximum lies at 620 nm and there is a significant increase in the molar absorption coefficient (Figure 3). The fluorescence maximum now appears at 635 nm, the spectral profile is much sharper than noted for EXP, and Φ_F approaches unity (Table 1). Similar changes are observed for the protonation of EXP–EXP and BOD–EXP. In the latter case, the presence of HCl has no effect on the optical properties of BOD. The absorption spectral profile of the diprotonated species EXP-($2H^+$) overlaps strongly with the fluorescence from BOD,

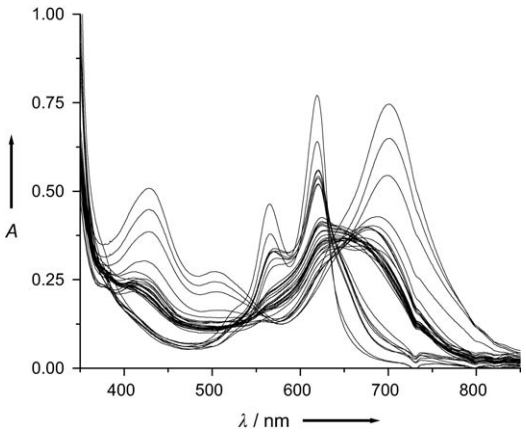

Figure 3. Spectrophotometric titration of BOD–EXP with HCl in CH_3CN, showing stepwise formation of the mono- and diprotonated species.

which leads to a fourfold increase in the overlap integral ($J_{DA} = 0.0056$ cm).

Quite unexpectedly, the rate of EET found for BOD–EXP($2H^+$) ($k_{EET} = 2.9 \times 10^9\ s^{-1}$) is only 20% higher than that determined for the neutral system. The experimental value for $|V_{CO}|$, calculated from Equation (1), falls to 0.70 cm^{-1}, which is approximately 60% of that derived for the neutral species. Protonation leads to a major disruption of the transition dipole moment on the acceptor, most notably by switching off the charge-transfer effect. This perturbs both the μ_A and κ^2 values relative to the neutral case. Calculation of the μ_A value from spectroscopic data,[14] however, shows that the change in this term is modest, with the actual value falling from 7.6 D to 6.8 D upon diprotonation. Because of the change in the nature of the absorption transition, more pronounced perturbations might be expected for the κ^2 value. Indeed, treatment of the transition moment vector as a simple point dipole leads to an estimate for κ^2 of 0.46, where the separation distance is 18.5 Å. By substituting these values into Equation 4, we calculate that $|V_{CO}| = (0.97 \pm 0.15)\ cm^{-1}$. Now the agreement is not so good and the calculation seems to overestimate the $|V_{CO}|$ value by a factor of around two.

Before attempting to improve this situation, attention was turned to the monoprotonated system EXP(H^+), formed during the early stages of the titration. For this species,[17] the absorption maximum occurs at 675 nm, while the fluorescence peak lies at 750 nm. The excited singlet state possesses increased charge-transfer character relative to EXP because of the inductive effect of the ammonium ion, but fluorescence is weak. The spectral overlap integral ($J_{DA} = 0.0023$ cm) lies between those of the neutral and dicationic forms. Because of the inherent asymmetry, the κ^2 value is difficult to compute and values range from 0.10 to 0.32. By taking the average value of $\kappa^2 = 0.21$, together with $R = 20.0$ Å and $\mu_A = 5.7$ D, we calculate that $|V_{CO}| = (0.20 \pm 0.14)\ cm^{-1}$. This value can be compared with that derived from the experimental rate constant ($k_{EET} = 5.8 \times 10^8\ s^{-1}$), which gives $|V_{CO}| = 0.46\ cm^{-1}$. It can be seen that both the relative uncertainty and the overall agreement have worsened considerably. This is undoubtedly due to the poor definition of the transition moment vector on the acceptor.

For the diprotonated species in BuCN containing excess HCl, there is a steady decrease in the k_{EET} value on cooling, which amounts to a twofold reduction in the k_{EET} value at 165 K. Furthermore, it was observed that the pK_{A2} value increases markedly as the temperature falls, whereas optical studies show that the monoprotonated species builds up in the absence of excess HCl. Similar behavior was noted for the monoprotonated species. The temperature dependence found for the k_{EET} value of all three forms of EXP can be well explained in terms of the change in line shape caused by modification of the dielectric properties of the solvent. Such behavior is consistent with the coulombic mechanism. Incidentally, this system functions as an excellent fluorescence-based thermometer in organic solvents.

The quality of agreement between computed and observed coupling elements is set by the distribution of the donor and acceptor wavefunctions. For BOD–EXP, the transition moment vectors are well-defined and, for the purpose of the computation, can be approximated as point dipoles. This is not so for EXP($2H^+$), where the wavefunction is "banana-like" and, given the relative proximity to the donor, should not be well defined as a single point. The situation is worsened for EXP(H^+), where the electronic system is best described as being of the push–pull–pull type because of the inductive effect of the ammonium ion. It is necessary to employ a more sophisticated treatment in these latter cases; this is made possible by using the transition density cube (TDC) approach.[18]

In this approach, the inverse products of wavefunctions computed at the CISD level[19] for the ground and singlet excited states of the donor and acceptor were used to represent the respective transition dipole densities. The computed values were normalized to the experimental transition dipole moments. Each transition density profile was arbitrarily broken down into 10 rectangles of equal area. Internal rotation around the spacer bonds has little real effect on the global value of κ^2 since the molecular axis is not changed. A refined value for $|V_{CO}|$ is then available by summation of all possible donor–acceptor interactions, with R being equated to the distance between centers of the respective boxes. The net result of this procedure was that the $|V_{CO}|$ value for the neutral D–Sp–A system hardly changed, the computed value being 1.07 cm^{-1}. The new value computed for the dicationic species BOD–EXP($2H^+$), $|V_{CO}| = 0.62\ cm^{-1}$, is much closer to the experimental value of $|V_{CO}| = 0.70\ cm^{-1}$ and appears to be a genuine improvement over the earlier estimate. It should be emphasized that the transition density, although curved, remains symmetric about the axis.

Application of the same strategy to BOD–EXP(H^+) resulted in a less satisfactory outcome, presumably because of the inherent asymmetry of the transition density. Here, the newly computed $|V_{CO}|$ value is 0.27 cm^{-1}, compared to the earlier calculated value of 0.20 and the experimental result of 0.46 cm^{-1}. This is certainly an improvement, which could be further refined using a 3D reaction field, and is probably within the reasonable limits for such calculations.

In conclusion, the quantitative agreement between computed and measured coulombic matrix elements for EET across 20 Å, where we might expect Förster theory to operate, depends markedly on the shape of the transition moment vectors. In an ideal case, agreement is within 25%, with the calculation underestimating the magnitude of $|V_{CO}|$. This level of agreement demands a very well defined vector and is not improved by using a more sophisticated treatment that allows for the 2D distribution of wavefunctions. For a poorly defined vector, the κ^2 value cannot be computed with any real significance by using point dipoles and the usual Förster-type approach cannot be relied upon to provide a realistic estimation of the $|V_{CO}|$ value. However, a marked improvement in the level of agreement between experimental and calculated matrix elements can be obtained by using a crude form of the TDC approach that allows for a 2D distribution of the wavefunctions. Indeed, for BOD–EXP($2H^+$) the computed $|V_{CO}|$ value is within 10% of the experimental value. Finally, the asymmetric transition density and strong charge-transfer character inherent to BOD–EXP(H^+) poses a severe test for Förster theory at short separations. The EXP(H^+) electronic system is of the push–pull–pull type and it is difficult to compute a reliable wavefunction for the excited state of the acceptor. Even so, the final agreement between experiment and calculation is reasonable. The net result is that Förster theory remains applicable to these closely spaced, intramolecular systems.

Received: January 12, 2009
Published online: March 13, 2009

Keywords: dyes/pigments · fluorescence · FRET · photochemistry · through-space interactions

[1] W. Kühlbrandt, D. A. Neng Wang, Y. Fujiyoshi, *Nature* **1994**, *367*, 614 – 621.
[2] S. Saini, H. Singh, B. Bagchi, *J. Chem. Sci.* **2006**, *118*, 23 – 35.
[3] a) V. Czikklely, H. D. Försterling, H. Kuhn, *Chem. Phys. Lett.* **1970**, *6*, 207 – 210; b) V. Czikkely, G. Dreizler, H. D. Försterling, H. Kuhn, J. Sondermann, P. Tillmann, J. Wiegand, *Z. Naturforsch. A* **1969**, *24*, 1821 – 1826.
[4] a) M. Isaksson, P. Hägglöt, P. Håkarsson, T. Ny, L. B.-Å. Johansson, *Phys. Chem. Chem. Phys.* **2007**, *9*, 3914 – 3922; b) C. Curutchet, B. Mennucci, G. D. Scholes, D. Beljonne, *J. Phys. Chem. B* **2008**, *112*, 3759 – 3766; c) S. E. Braslavsky, E. Fron, H. B. Rodríguez, E. San Romáin, G. D. Scholes, G. Schweitzer, B. Valeur, J. Wirz, *Photochem. Photobiol. Sci.* **2008**, *7*, 1444 – 1448.
[5] a) K. F. Wong, B. Bagchi, P. J. Rossky, *J. Phys. Chem. A* **2004**, *108*, 5752 – 5763; b) R. E. Dale, J. Eisinger, W. E. Blumberg, *Biophys. J.* **1979**, *26*, 161 – 194.
[6] A. Juris, L. Prodi, A. Harriman, R. Ziessel, M. Hissler, A. Elghayoury, F. Wu, E. C. Riesgo, R. P. Thummel, *Inorg. Chem.* **2000**, *39*, 3590 – 3598.
[7] F. Thiemann, T. Piehler, D. Haase, W. Saak, A. Lützen, *Eur. J. Org. Chem.* **2005**, 1991 – 2001.
[8] W. W. Qin, M. Baruah, M. Van der Auweraer, F. C. De Schryver, N. Boens, *J. Phys. Chem. A* **2005**, *109*, 7371 – 7384.
[9] M. Baruah, W. W. Qin, C. Flors, J. Hofkens, R. A. L. Vallée, D. Beljonne, M. Van der Auweraer, M. De Borggraeve, N. Boens, *J. Phys. Chem. A* **2006**, *110*, 5998 – 6009.
[10] D. Beljonne, G. Pourtois, C. Silva, E. Hennebicq, L. M. Herz, R. H. Friend, G. D. Scholes, S. Seteyesh, K. Müllen, J. L. Brèdas, *Proc. Natl. Acad. Sci. USA* **2002**, *99*, 10982 – 10987.
[11] P. D. Laible, R. S. Knox, T. G. Owens, *J. Phys. Chem. B* **1998**, *102*, 1641 – 1648.
[12] B. P. Krueger, S. S. Lampoura, I. H. M. van Stokkum, E. Papagiannakis, J. M. Salverda, C. C. Gradinaru, D. Rutkauskas, R. G. Hiller, R. van Grondelle, *Biophys. J.* **2001**, *80*, 2843 – 2855.
[13] G. D. Scholes, X. J. Jordanides, G. R. Fleming, *J. Phys. Chem. B* **2001**, *105*, 1640 – 1651.
[14] R. G. Alden, E. Johnson, V. Nagarajan, W. W. Parson, C. J. Law, R. G. Cogdell, *J. Phys. Chem. B* **1997**, *101*, 4667 – 4680.
[15] G. Hungerford, M. Van der Auweraer, J.-C. Chambron, V. Heitz, J.-P. Sauvage, J.-L. Pierre, D. Zurita, *Chem. Eur. J.* **1999**, *5*, 2089 – 2100.
[16] During the titration, an irreversible side product that absorbs at ca. 570 nm accumulates in solution.
[17] R. Ziessel, G. Ulrich, A. Harriman, M. A. H. Alamiry, B. Stewart, P. Retailleau, *Chem. Eur. J.* **2009**, *15*, 1359 – 1369
[18] B. P. Krueger, G. D. Scholes, G. R. Fleming, *J. Phys. Chem. B* **1998**, *102*, 5378 – 5386.
[19] TURBOMOLE; R. Ahlrichs, M. Bär, M. Häser, H. Horn, C. Kölmel, *Chem. Phys. Lett.* **1989**, *162*, 165 – 169.
[20] A. Harriman, L. J. Mallon, R. Ziessel, *Chem. Eur. J.* **2008**, *14*, 11461 – 11473.

